J. Phys. IV France 11 (2001)

Quenching and ageing behaviour of quaternary Cu-Zn-Al-Ni single crystals

E. Zelaya[1], J.L. Pelegrina[1,2] and M. Ahlers[1,3]

Universidad Nacional de Cuyo, Centro Atómico Bariloche, 8400 S.C. de Bariloche, Argentina
[1] *CONICET, Centro Atómico Bariloche, 8400 S.C. de Bariloche, Argentina*
[2] *Comisión Nacional de Energía Atómica, Centro Atómico Bariloche, 8400 S.C. de Bariloche, Argentina*

Abstract. The ageing behaviour of the martensite in single crystals made from the quaternary alloy (Cu - 9.04 at%Zn - 20.87 at%Al - 3.07 at%Ni) was investigated, together with a characterization of the structure and the microstructure in the initial condition. The long range ordering temperatures were determined by electrical resistivity measurements. The stabilization of stress induced martensite was quantitatively studied as a function of time and temperature. After performing the same thermal treatment as for the ageing experiments, slices for transmission electron microscopy were cut and the resulting structure and microstructure were analyzed. The high temperature β phase is long range ordered and the martensite has the 18R structure. No evidence for the appearance of γ precipitates was found after a quench from 770 K. However, a large number of vacancy loops with straight borders lying in {1 0 0} planes were present, with the corresponding dislocations dissociated in partials. It was also found that the stabilization process takes place in the martensite, but with a slower kinetics than in Cu-Zn-Al.

1. INTRODUCTION

The 18R martensite of Cu-Zn-Al alloys is found to stabilize during ageing. The consequences of this stabilization are reflected in different ways, depending on the method the transition is induced [1]. The increase in transformation temperatures in stress free experiments and the decrease of the transformation stresses at constant temperature are the best known effects. It has been proposed that the vacancy assisted interchange of certain Cu and Zn atoms is the process that occurs during the martensite ageing [2], altering the long range order inherited from the high temperature β phase and being responsible for the lowering of the free energy of the system.

On searching for applications, Cu-Al-Ni alloys have demonstrated to have a better thermal stability than the Cu-Zn-Al ones. The stabilization occurs at higher temperatures and is followed by the decomposition to the equilibrium phases [3]. One of these phases, which is denoted as γ, also appears in the Cu-Zn-Al alloys studied in [2], and is a consequence of the thermal treatment used to enhance the stabilization in the experiments. Notwithstanding, at lower temperatures a degradation of the two way shape memory effect occurs [4], due to the volume increase of 2H martensite with ageing, at the expense of the 18R structure, a phenomenon which does not occur in Cu-Zn-Al. Therefore, it was found of interest to analyze a quaternary Cu-Zn-Al-Ni alloy, with intermediate compositions of Zn and Al, searching for the improvement of the ageing stability. The results of the structure and microstructure, as also the behaviour of the stress induced transformation with time are reported in this paper.

2. EXPERIMENTAL PROCEDURES

A Cu - 9.04 at%Zn - 20.87 at%Al - 3.07 at%Ni alloy (electron concentration: e/a = 1.496) was prepared from high purity metals. Due to its high melting temperature, the Ni was alloyed first with the Cu pieces by arc melting in an Ar atmosphere. After several remeltings, the resulting button was cut and its homogeneity was analyzed by energy dispersive spectroscopy in a scanning electron microscope. The Al, Zn and Cu-Ni pieces were melted together in sealed quartz tubes in an Ar atmosphere using now a resistance furnace. Single crystals of the β phase with a 6 mm diameter were then grown by the Bridgman technique and left at 1070 K for two days to improve homogenization. Subsequently their orientations were determined by the Laue X-ray method.

Three samples for the tensile experiments were spark machined with a central cylindrical part of around 13 mm length and 3 mm diameter. Before each stabilization experiment, the samples were homogenized at 1070 K for 600 s, air cooled to 770 K and quenched into water at room temperature. Then each sample was inserted into the deformation machine and kept at the working temperature for 180 s. Afterwards the stabilization experiments were performed in the same way as in [2], using an Instron 5567 machine with a temperature module and at a strain rate of 1.3×10^{-4} s^{-1}.

In some of the samples, resistivity measurements were performed by the four terminal method to obtain the characteristic transformation temperatures and the temperature of ordering. Typical scanning rates were around 5 K / s for the former and 50 K / s for the latter.

Samples for transmission electron microscopy were cut from cylinders of 3 mm diameter after the different thermal treatments. The samples were electropolished until perforation, as done in [5]. The observations were made in a Philips EM300 at an accelerating voltage of 100 kV, using a double tilt specimen holder.

3. RESULTS AND DISCUSSION

3.1 Structure

The Laue photographs taken from the single crystals at room temperature present spots that agree with those observed for the β phase of Cu-Zn-Al alloys. Resistivity measurements have been performed to determine the presence of ordering reactions, as shown in Fig. 1. The alloy was found sufficiently stable under the experimental conditions and no decomposition was detected. It can be also noted in the figure that a small hysteresis is present, its origin is probably associated with the speed of temperature cycling necessary to avoid decomposition. In order to better locate the ordering temperatures, the curve was smoothed by doing an adjacent averaging of the experimental data, and the result plotted as a function of time as shown in Fig. 2 for the cooling branch. There the two ordering transitions can be clearly seen (compare with Fig. 1) and they agree with those obtained in the same way during the heating. Their mean values are 850 K for B2 order and 720 K for $L2_1$ order. In comparison, for a Cu-Zn-Al alloy of e/a =1.48 and a similar Zn concentration, the ordering temperatures were 775 K and 710 K respectively [6]. On the other hand, for Cu - 26.0 at%Al - 3.7 at%Ni the values of 813 K and 773 K had been obtained [7].

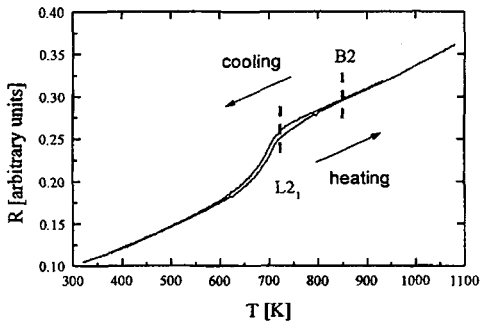

Figure 1: Electrical resistance versus temperature. The cooling curve follows the heating one.

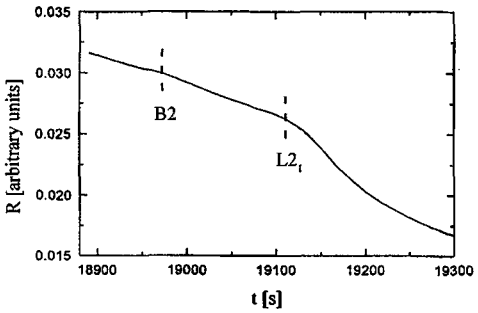

Figure 2: Electrical resistance versus time in the cooling branch.

In Table 1 are listed the data of the samples used in the stabilization experiments. The mean values of the stress free transformation temperatures M_S can be compared with empirical relations available from the literature. In [8, 9] the influence on M_S by the addition of small concentrations of a third element was determined, whereas in [10] quaternary alloys were analyzed. The present experimental results show a difference with these relations, being lower by around 40 K and higher by 70 K, respectively. The discrepancies are explained by changes in the nominal composition in the former case, whereas in the latter instance only commercially pure materials were used.

Table 1: Samples used in tension experiments, transformation temperature at zero applied stress (M_S), tensile axis orientation and corresponding Schmid factor for the transformation $\beta \rightarrow \beta'$.

Sample	M_S [K]	Tensile axis	Schmid factor
1	264	[0 1 10]	0.492
2	253	[0 1 10]	0.492
3	233	[2 3 12]	0.484

3.2 Ageing experiments

In Fig. 3 is shown a typical stress strain curve, in which the partially transformed martensite was stabilized at T_S during a time t_S. It can be seen that the hysteresis width increases with t_S in the transformed zone, compared to a smaller and constant value (within experimental scatter) in the nonstabilized zone. The latter value is equal to the hysteresis width of a sample which has reached equilibrium after the thermal treatment. That at the release of the load the deformation does not return to the initial value is a consequence of the accommodation of the heads of the sample to the grips of the deformation machine.

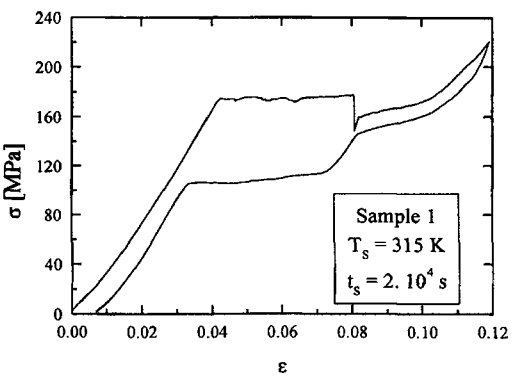

Figure 3: Typical shape of the applied stress versus deformation curve in a stabilization experiment.

The samples were stabilized at several temperatures T_S = 295, 305 and 315 K, and the difference in the hysteresis width after stabilization with respect to the nonstabilized value was taken as the stress shift $\Delta\sigma$. Using the stress shift $\Delta\sigma$ and the corresponding Schmid factor (Table 1) the difference in resolved stress $\Delta\tau$ was calculated and plotted as a function of the stabilization time in Fig. 4. It can be seen that the $\Delta\tau(t)$ behaviour is similar to that found for Cu-Zn-Al alloys, although slower and shifted by three orders of magnitude to larger times. Due to this reduced stabilization, it was not possible to reach a saturation value as in [2, 11]. Within experimental scatter, a unique slope at the linear portion of largest increase can be determined for the three stabilization temperatures, resulting in an average value of $d\,\Delta\tau / d \ln t = 11.8$ MPa, as shown by the dashed lines in Fig. 4. Their extrapolation to the $\Delta\tau = 0$ value (dotted line in Fig. 4) permitted to determine the times t_0, which as a function of T_S^{-1} are plotted in Fig. 5. From the slope of this figure an activation energy of (117 ± 8) kJ / mol is deduced for the stabilization process, which is definitely higher than the (97 ± 7) kJ / mol obtained for Cu-Zn-Al [2]. According to [12], the vacancy formation energy is a smooth linear function of the electron concentration, implying that for the ternary and quaternary alloys under comparison, no significant differences in the vacancy concentration at the quenching temperature are to be expected. Therefore, considering the same vacancy concentration in the model of [2], the activation energy difference alone can explain the reduced ageing

activity of the present alloy. This fact holds even taking into account a vacancy concentration reduction in the martensite, similar to that measured during the ageing of the β phase [13].

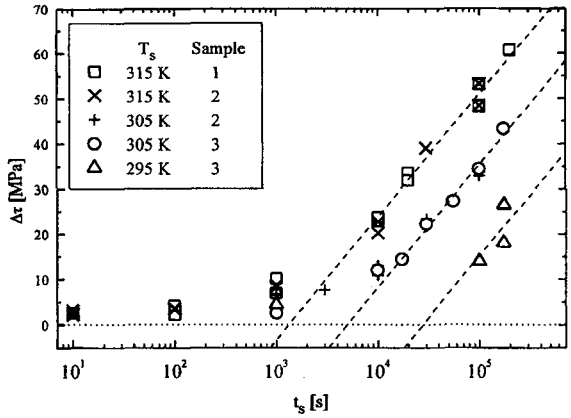

Figure 4: Resolved stress shift versus stabilization time for three samples and several working temperatures T_S. The dashed lines correspond to the least square fit of the region of largest increase, and the dotted line is $\Delta\tau = 0$.

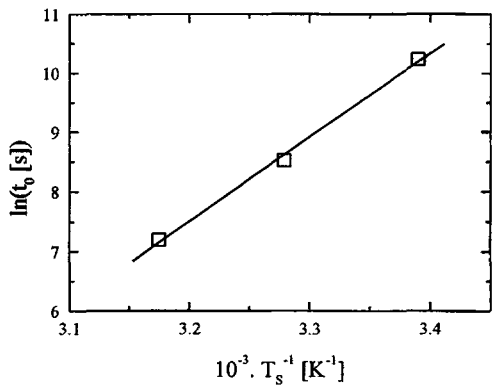

Figure 5: Time t_0 from linear extrapolation of the curves in Fig. 4 to $\Delta\tau = 0$ versus the inverse of the stabilization temperature T_S.

3.3 Microstructure

Since the stabilization is a process that requires the presence of vacancies, a special heat treatment was performed in [2] to increase their concentration. In order to compare with those results, the same treatment was applied to the present alloy. Therefore, it is of interest to observe the consequences of this thermal treatment, to allow also the comparison with previous results. In [2], small γ precipitates were reported to appear after the quench, acting as sinks for the vacancies since they form a stable part of its structure. Each unit cell has two structural vacancies and a typical cubic precipitate with sides around 40 nm [14] consumes nearly such 2. 10^5 defects.

In Fig. 6 can be seen the microstructure of a sample in the β phase quenched from 770 K into water at room temperature. Several large dislocation loops or networks (around 800 nm x 800 nm) can be observed separated by a distance of around 5 μm from each other. The photographs were taken with the foil normal to [001] and the dislocations extended mainly in [100] (Fig. 6 b) and [010] (Fig. 6 c). It was found that the dislocations have an edge character with a Burgers vector of the type [001]. By tilting into the [102] zone axis and comparing the bright field images taken under two beam condition with positive

and negative diffracting vector g (g = -4 2 2) and positive deviation parameter s, it was possible to determine the image side of the dislocations, from which it was concluded that they arose from the collapse of vacancies on the (001) plane (i.e. vacancy loops). From Fig. 6 it can also observed that the dislocations are split into partials with the same 1/2 [001] Burgers vector.
Square dislocation loops, with the same Burgers vector and arising from the collapse of vacancies have been found in other Cu based alloys, although not as extended. They were obtained in Cu-Zn by zinc-loss annealing [15, 16], as also after quenching [17, 18], or in explosively deformed samples [19]. It was demonstrated that this type of dislocation shows a directional instability due to the anisotropy of the material [16], and that this is the reason to adopt the <100> line directions. Similar loops were found in Cu-Al-Ni after quenching [20], but with a fringe contrast attached to them. No dissociation was reported.

(a) (b) (c)

Figure 6: Bright field electron micrographs in two beam condition for the vacancy loops in (001): (a) g = -2 2 0; (b) g = 0 4 0; (c) g = 400. The direction which becomes invisible is parallel to the corresponding active g. The bar denotes 800 nm.

An estimation of the amount of vacancies that were necessary to form such loops can be made, considering the size of the network and the lattice spacing of the $L2_1$ ordered β phase, $a_\beta \approx 6$ Å [21]. If a simple loop of 14000 Å x 11000 Å is considered, similar in size as that shown in Fig. 6, more than 68. 10^6 vacancies are required to collapse. By considering the mean separation of the loops, the vacancy consumption is equivalent to a concentration of 7.8 10^{-6}. The sample was air cooled from 1070 K to 770 K in approximately 180 s, being slow enough to suppose that the sample is close to thermal equilibrium. Using a vacancy formation energy of 0.57 eV and an entropy of 1.6 k_B (k_B Boltzmann constant) [13], an equilibrium concentration of 9.2 10^{-4} at 770 K is obtained. When this quantity is compared with that precipitated in the loop, it can be concluded that most of the vacancies existing in equilibrium at 770 K remains in solution after quenching. This conclusion agrees with the measurements of the initial concentration of quenched-in vacancies in Cu-Zn-Al alloys [13], resulting 7.5 10^{-4} for an alloy of near Zn and Al concentrations. This further substantiate the assertion that it is the change in activation energy and not a decrease in vacancy concentration after quenching which is responsible for the lower stabilization in Cu-Zn-Al-Ni compared to Cu-Zn-Al.

4. CONCLUSIONS

Single crystals of the quaternary Cu - 9.04 at%Zn - 20.87 at%Al - 3.07 at%Ni alloy (e/a = 1.496) were analyzed.
a- The alloy transforms from the β phase to the 18R martensite at M_S temperatures around 249 K.
b- The β phase presents two ordering transitions: A2 → B2 at 850 K and B2 → $L2_1$ at 720 K.
c- The martensite stabilizes during ageing at temperatures in the range (295 K - 315 K), after a quench from 770 K.
d- An activation energy of the stabilization process of (117 ± 8) kJ / mol was determined, greater than for the ternary Cu-Zn-Al alloys.

e- The presence of vacancy loops in the β phase and the absence of γ precipitates after the thermal treatment was verified.
f- The slower stabilization in Cu-Zn-Al-Ni compared to Cu-Zn-Al is suggested to be caused solely by the higher activation energy for the vacancy movement.

Acknowledgments

This work was supported by the ANPCyT, CNEA and CONICET, Argentina.

References

1. M. Ahlers, Proc. ICOMAT 86, Jpn. Inst. Metals, 786 (1986).
2. A. Abu Arab, M. Ahlers, Acta metall. 36, 2627 (1988).
3. V. Pelosin, A. Rivière, J. Alloys and Compounds 268, 166 (1998).
4. H. Morawiec, M. Gigla, J. de Phys. IV 5, C8-937 (1995).
5. J.L. Pelegrina, M. Chandrasekaran, M.S. Andrade, Acta metall. 36, 1111 (1988).
6. R. Rapacioli, M. Ahlers, Scripta metall. 11, 1147 (1977).
7. I. Hurtado, D. Segers, J. Van Humbeeck, L. Dorikens-Vanpraet, C. Dauwe, Scripta metall. mater. 33, 741 (1995).
8. H. Pops, Trans. AIME 236, 1532 (1966).
9. H. Pops, N. Ridley, Met. Trans. 1, 2653 (1970).
10. N. Mwamba, L. Delaey, J. de Phys. 43, C4-639 (1982).
11. M. Stipcich, R. Romero, Mat. Sci. and Eng. A273-275, 581 (1999).
12. H. Fukushima, M. Doyama, J. Phys. F: Metal Phys. 9, L177 (1979).
13. R. Romero, A. Somoza, Mat. Sci. and Eng. A273-275, 572 (1999).
14. F.C. Lovey, G. Van Tendeloo, J. Van Landuyt, M. Chandrasekaran, S. Amelinckx, Acta metall. 32, 879 (1984).
15. A.J. Morton, Phil. Mag. A 50, 797 (1984).
16. A.J. Morton, Phil. Mag. A 52, 99 (1985).
17. S.G. Cupschalk, N. Brown, Acta metall. 15, 847 (1967).
18. H. Yamaguchi, S. Ishii, Y. Nakane, S. Yoshida, Jpn. J. Appl. Phys. 20, 1191 (1981).
19. J.V. Rinnovatore, N. Brown, Trans. AIME 239, 225 (1967).
20. N. Zárubová, A. Gemperle, V. Novák, J. de Phys. IV 7, C5-281 (1997).
21. S. Chakravorty, C.M. Wayman, Acta metall. 25, 989 (1977).